# Double layer printed high performance OLED based on PEDOT:PSS/ $Ir(bt)_2acac$:CDBP

Cite as: AIP Advances **8**, 115112 (2018); https://doi.org/10.1063/1.5053133
Submitted: 21 August 2018 . Accepted: 26 October 2018 . Published Online: 07 November 2018

Wanying Mu, Tong Lin, Yongxu Hu, Yuling Sun, Zhenzhen Du, Jing Jin, Dongyu Zhang, and Zheng Cui

# Double layer printed high performance OLED based on PEDOT:PSS/Ir(bt)$_2$acac:CDBP

Wanying Mu,[1,2] Tong Lin,[2,3] Yongxu Hu,[2,4] Yuling Sun,[2] Zhenzhen Du,[2] Jing Jin,[1] Dongyu Zhang,[2,a] and Zheng Cui[2]
[1]*College of Materials Science and Engineering, Shanghai University, Shanghai 200444, China*
[2]*Printable Electronics Research Center, Suzhou Institute of Nano-Tech and Nano-Bionics, Chinese Acedemy of Science, 398 Ruoshui Road, Suzhou Industrial Park, Suzhou, Jiangsu 215123, People's Republic of China*
[3]*State Key Laboratory of Luminescence and Applications, Changchun Institute of Optics, Fine Mechanics and Physics, Chinese Academy of Sciences, Changchun 130033, PR China*
[4]*School of Chemical Engineering, University of Science and Technology Liaoning (USTL), Anshan 114051, People's Republic of China*

(Received 21 August 2018; accepted 26 October 2018; published online 7 November 2018)

The preparation of organic electroluminescent diodes (OLEDs) by printing with the potential advantages of high material utilization, low equipment cost, simple process flow, and favorable for large-area device preparation, is expected to be the next generation of OLED fabrication method. In this paper, PEDOT: PSS and CDBP: Ir(bt)$_2$acac functional layers were prepared by spin coating/printing and characterized, respectively. The results show that the double layer printing device achieved the best performance, the maximum brightness and external quantum efficiency reach 4357cd/m$^2$ and 2.45%, even better than that of the spin coated reference. It indicates that the ink-jet printing process has a potential to overwhelm the spin-coating one for constructing high performance OLED.  https://doi.org/10.1063/1.5053133

## I. INTRODUCTION

After C. W. Tang et al invented the organic light-emitting diode device (OLED) and followed by nearly 30 years of development, OLED technology has finally been accepted by display industry.[1–6] Currently, the dominant industrial manufacturing process for OLED display panels is thermal evaporation. Because of the much less material utilization, complex process flow, high equipment cost[7] and difficulty to guarantee the uniformity of large-area devices, this route has led to high cost of OLED panels and limited the market penetration. In contrast, fabrication of OLED panels by printing is an atmospheric process, with high utilization of materials and low production cost, which has generated significant interests from the scientific community and industry.

At present, a number of printing processes including spin coating,[8] gravure printing,[9] screen printing,[10] and inkjet printing[11] have been used for OLED fabrication. Among them, inkjet printing featuring as non-contact, mask less, digital fabrication and high precision,[12] have become the favorite technology. Significant progresses have been made for inkjet printing OLED over the years.[13–18] However, the current academic laboratory results are mostly based on printing only one functional layer. And according to the industrial OLED technology roadmap, it is expected that from the hole injection (HIL) to the emitting layer (EML) can be printed.

Compared with the vacuum thermal evaporation process, in the process of multilayer printing, the interface between different functional layers, mutual solubility of solvents, functional

[a]dyzhang2010@sinano.ac.cn

 

ink spreading, film formation and uniformity control, etc. become more complex and difficult to control, caused the lower device performance even inferior to the corresponding spin-coated devices. In order to explore those problems which could happened in multilayer printing procedure, poly 3,4-ethylenedioxythiophene: polystyrene sulfonate (PEDOT: PSS) and bis (2-phenyl-1,3-benzothiozolato-N,C2') iridium (acetylacetonate) ($Ir(bt)_2(acac)$):9-[4-(4-carbazol-9-yl-2- methylphenyl)-3-methylphenyl] carbazole(CDBP) were chosen as HIL and EML, printing and spin-coating methods were used to construct them in this article, respectively. Finally, the double layer printed OLED devices achieved the superior performance to that of spin-coated one, which provided a strong support for the bright future of all printing OLED technology.

## II. EXPERIMENTAL

### A. Materials and instruments

PEDOT: PSS (Clevios 4083) was used as the hole injection layer, and CDBP doped with $Ir(bt)_2acac$ (mass ratio of 9:1) were used as the light-emitting layer. For inkjet printing, the butyl benzoate was used as the solvent and the concentration was 30 mg/ml. For spin-coating, chlorobenzene was used as the solvent with the concentration of 15 mg/ml. 1,3,5-tris(1-phenyl-1H-benzimidazol-2-yl)benzene (TPBi) was used as the electron transport layer (ETL), 8- Hydroxyquinoline Lithium ($Liq_3$) as electron injection layer (EIL), and Al as cathode. TPBi, CDBP and $Ir(bt)_2acac$ were purchased from Xi'an Baolaite Photo-Electric Technology Co., Ltd. and The molecular structures of functional materials used in this work are shown in Figure 1.

PEDOT: PSS and CDBP: $Ir(bt)_2acac$ functional layers were printed by Fujifilm Dimatix 2850. The ETL/EIL/Al were deposited by vacuum thermal deposition system. Electroluminescence properties of four OLED devices were measured using Keithley 2400 Source Meter current-voltage source meter and PR655 photometer, BM-7 photoelectric comprehensive measurement system in air. Thicknesses of functional layers were obtained by profile meter (DektakXT, BRUKER). AFM images were collected using Dimension 3100 (Veeco, America).

### B. Fabrication of OLED devices

The OLED device structure is shown in Fig. 2. It was made on indium tin oxide (ITO) coated glass substrates. The ITO substrate was cleaned with a glass cleaner, ethanol and acetone, and then deionized water, ethanol, and acetone were sequentially ultrasonicated for 10 min. After drying, oxygen plasma treatment was performed for 3 minutes. The PEDOT: PSS and CDBP: $Ir(bt)_2acac$ were sequentially deposited by either inkjet printing or spin coating at different thicknesses as listed

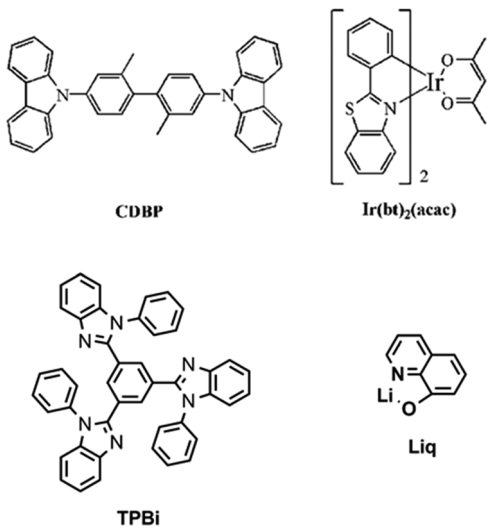


FIG. 1. Molecular structures of materials for the OLEDs.

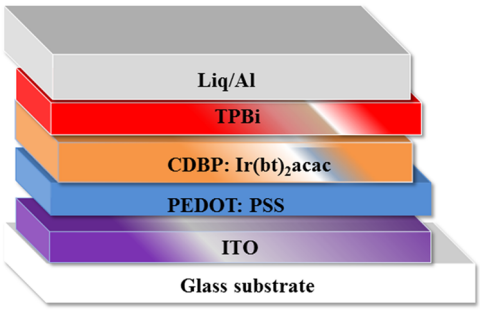


FIG. 2. Schematic of OLED device layer structure.

TABLE I. Thickness of PEPOT:PSS and CDBP:Ir(bt)$_2$acac during printing and spin coating.

| | PEPOT:PSS | CDBP:Ir(bt)$_2$acac |
|---|---|---|
| Spin-coating | 26nm | 25nm |
| Printing | 24nm | 28nm |

TABLE II. The design of OLED device.

| Device | PEDOT: PSS | CDBP: Ir(bt)$_2$acac |
|---|---|---|
| A | Spin-coating | Spin-coating (solvent: chlorobenzene, concentration:15mg/mL) |
| B | Spin-coating | Inkjet printing (solvent: butyl benzoate, concentration: 30mg/mL) |
| C | Inkjet printing | Spin-coating (solvent: chlorobenzene, concentration:15mg/mL) |
| D | Inkjet printing | Inkjet printing (solvent: butyl benzoate, concentration: 30mg/mL) |

in Table I. The TPBi (30 nm)/Liq (2 nm)/Al (100 nm) was sequentially deposited by vacuum thermal evaporation. In order to investigate the influence of different solution deposition processes on the multi-layer OLED devices, both spin coating and inkjet printing processes were performed and four groups of devices were made, as shown in Table II, and characterized.

All the spin coating processes were at 4000 rpm for 30s, and the inkjet printing processes were performed with 10pl cartridge using Dimatix 2850. The coated PEPOT: PSS film was baked on a hot plate at 120°C for 15 min, and EML film was baked at 60°C for 15min.

## III. RESULTS AND DISCUSSION

The electroluminescent properties of device A and device B are shown in Fig. 3. The maximum luminance, current efficiency, power efficiency and external quantum efficiency (EQE) of device A are 2264 cd/m$^2$, 6.638 cd/A, 2.35 lm/W and 2.3%, respectively. These parameters for Device B are 1201 cd/m$^2$, 6.445 cd/A, 3.15 lm/W and 2.14%.

For device C, the maximum luminance, current efficiency, power efficiency and EQE are 2033 cd/m$^2$, 4.886 cd/A, 2.19 lm/W, and 1.62%, respectively. These Parameters for device D are 4357 cd/m$^2$, 7.318 cd/A, 3.54 lm/W and 2.45%. They are shown in Fig. 4. The actual data are given in Table III.

As the EL spectrum shown in Figure 4(d), all of the four devices emit the same spectrum. The emission peaks at 560 nm, regardless of spin coated or inkjet printed. It is apparent that different solvents and coating methods have no influence on emitting material.

As the data shown in Table III, the inkjet printed device D achieved the best performance among the four devices with the highest luminance, the lowest turn-on voltage and the best efficiency. Since the film obtained by both spin coating and printing processes kept almost the same thickness as shown in Table I, the probability of performance difference caused by different film thickness can be

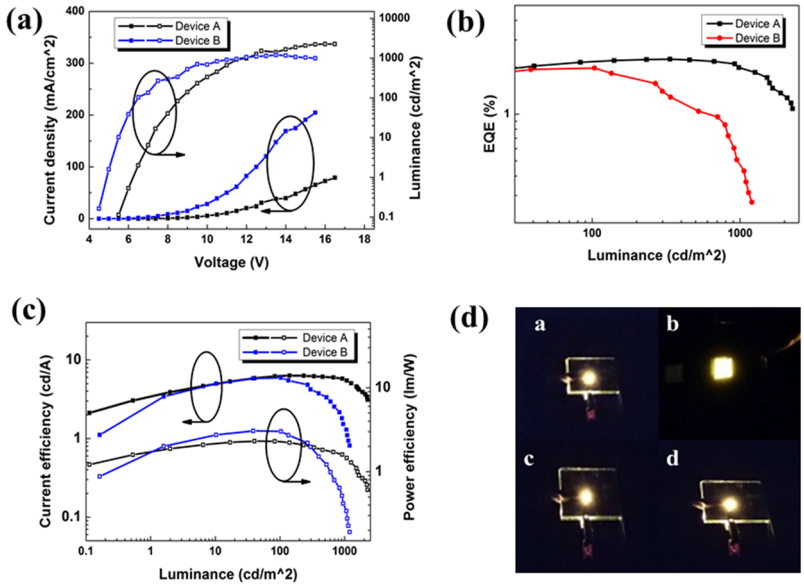


FIG. 3. (a)V-J-L curves; (b) L-EQE curses; (c) L-C.E-P.E curves of Device A and Device B; (d) illuminated diagram of four devices.

excluded. Further investigation of film morphology by AFM showed that all of those double layers have almost identical morphology and roughness, as the AFM images of HIL/EML shown in Figure 5.

The surface energy of PEDOT: PSS layer was also investigated by measuring the contact angle, in order to determine the interface property after deposition of CDBP: $Ir(bt)_2acac$ layer. It is very interesting to find that the inkjet printed PEDOT: PSS film has larger contact angle than spin coated film, but it is the opposite for EML, as shown in Figure 6. This may explain why the all-printed device D has the best property compared to other devices.

When a liquid is deposited by inkjet printing or spin coating, different forces are exerted to the molecules in the liquid. It is obvious that spin coating generates much larger centrifuge force whereas inkjet printing does not. This force can have influence on the molecular arrangement,[19,20] which will affect the spreading of the next layer and hence the interface property. It is known that the

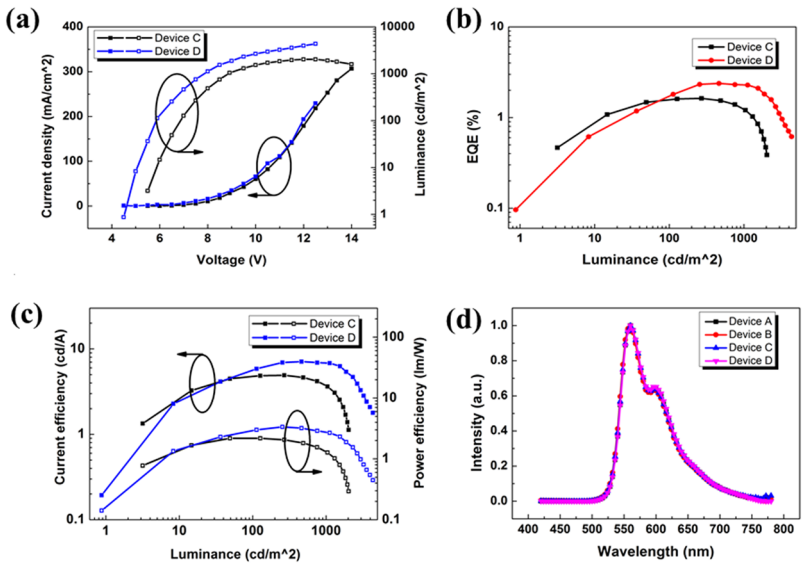


FIG. 4. (a) V-J-L curves; (b) L-EQE curses; (c) L-C.E-P.E curves of Device C and Device D; (d)Spectrum of four devices.

TABLE III. Electroluminescence properties of four OLED devices. $V_{on}$: the voltage at 1 cd $m^{-2}$.

| | | At 200cd $m^{-2}$ | | | | | maximum values | | | |
|---|---|---|---|---|---|---|---|---|---|---|
| | $V_{on}$ | Voltage (V) | CE (cd $A^{-1}$) | PE (lm $W^{-1}$) | EQE (%) | CIE (x,y) | L (cd $m^{-2}$) | CE (cd $A^{-1}$) | PE (lm $W^{-1}$) | EQE (%) |
| Device A | 5.9 | 9.5 | 6.6 | 2.2 | 2.3 | (0.51,0.48) | 2264 | 6.638 | 2.35 | 2.30 |
| Device B | 5.0 | 7.2 | 5.0 | 2.1 | 1.7 | (0.48,0.50) | 1201 | 6.445 | 3.15 | 2.14 |
| Device C | 5.0 | 7.2 | 4.8 | 2.1 | 1.6 | (0.49,0.50) | 2033 | 4.886 | 2.19 | 1.62 |
| Device D | 4.5 | 6.3 | 5.3 | 2.7 | 1.8 | (0.50,0.50) | 4357 | 7.318 | 3.54 | 2.45 |

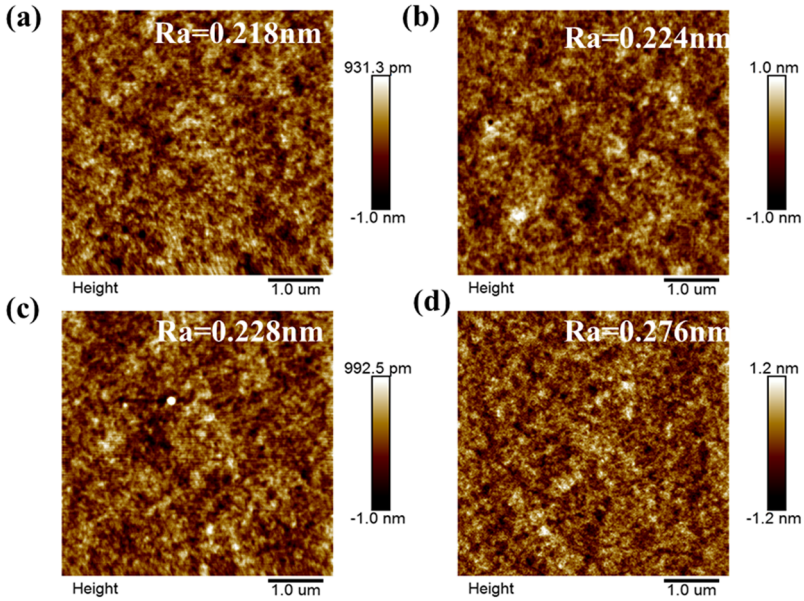


FIG. 5. The AFM images of (a) spin coating HIL/spin coating EML (S+S); (b) spin coating HIL/printing EML (S+P); (C) printing HIL/spin coating EML (P+S); (D) printing HIL/printing EML (P+P).

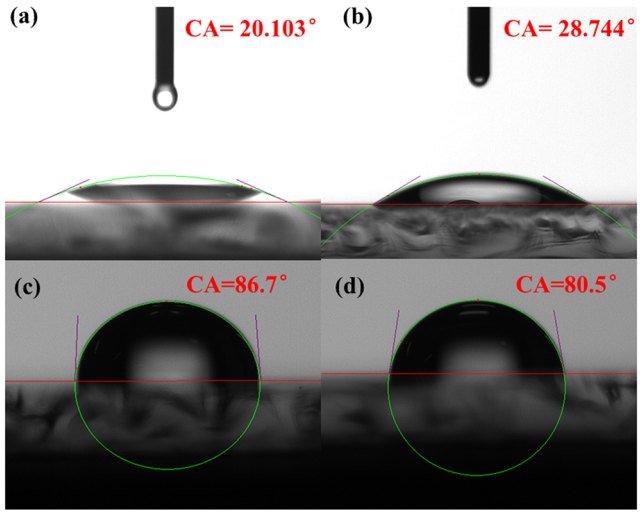


FIG. 6. The contact angles of water drop on (a)spin-coated PEDOT:PSS; (b)printed PEDOT:PSS; (c) spin-coated EML; (d) printed EML.

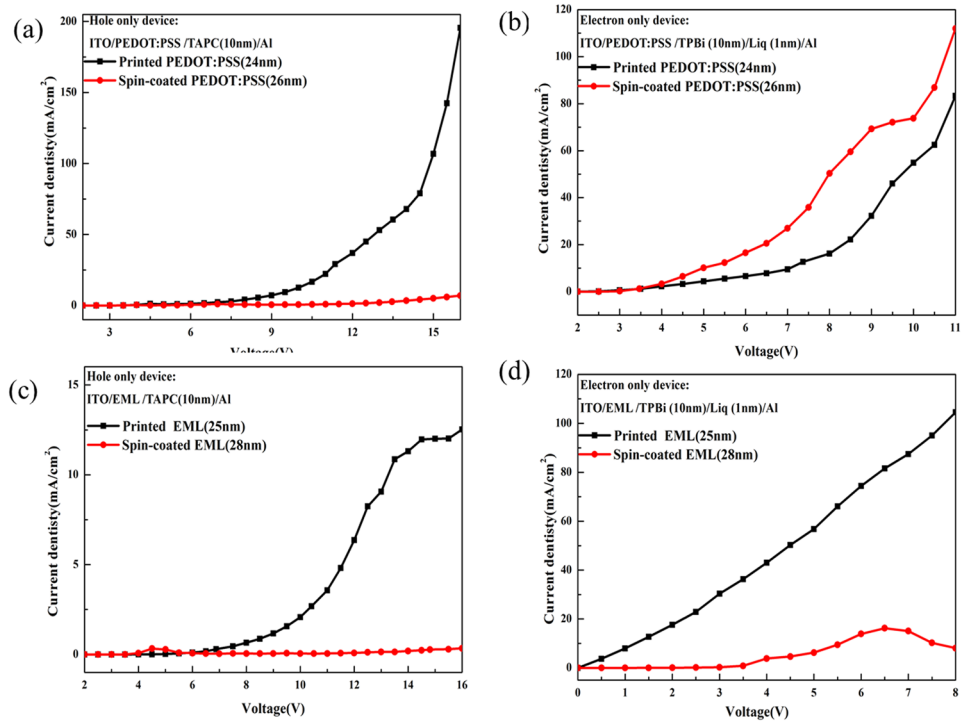


FIG. 7. The V-J curves of single carrier devices.

interface property between functional layers plays a critical role to balance the carrier mobility.[21–24] To verify this hypothesis, a series of single charge carrier printed/spin-coated devices were made and characterized. In detail, ITO/HIL or EML (24~28nm)/TAPC (10nm)/Al and ITO/HIL or EML (24~28nm)/TPBi (10nm)/Liq (1nm)/Al are designed as hole only and electron only device to explore the effect of printing and spin coating process on the charge transport ability of HIL/EML, respectively. From the result as shown in Figure 7, we can found both of the printed HIL and EML exhibit higher charge transport ability in hole only devices. The lower hole transport ability exhibited in spin-coated HIL and EML means a higher voltage is needed to drift the charge from ITO into HIL and generate exciton in EML. As a result, a high bias should be applied in Device A to achieve the same luminescence as its reference item. For electron only devices group, the printed and spin coated HIL show comparative charge transport ability. On the other hand, the printed EML shows higher electron transport ability than spin coated one. As we know, a higher hole and lower electron transport ability of printed PEDOT:PSS is beneficial to confine the exciton placed in EML. At the same time, a higher electron transport ability of printed EML assures more balance carrier happened than spin-coated one. Both of them contribute to the best performance of double layer printed device.

## IV. CONCLUSIONS

In this paper, we constructed four OLED devices in which the PEDOT: PSS and CDBP: $Ir(bt)_2acac$ functional layers were prepared by spin coating and printing, respectively. The double-layer printing device got the most brilliant performance in them, the maximum brightness, current efficiency, power efficiency and EQE reached 4357 cd/m$^2$, 7.318 cd/A, 3.54 lm/W and 2.45%. We attribute the high performance comes from a higher hole and lower electron transport ability of printed PEDOT: PSS combining with a higher electron transport ability of printed EML. With the help of them, more balance carriers and exciton confining can be obtained in EML, and the better performance than the spin coated reference can be achieved. This work provides a strong support for the bright future of all printing OLED technology.

## ACKNOWLEDGMENTS

This research was funded through National Key Research and Development Program of China (Project No. 2017YFB0404403).

[1] C. W. Tang and S. A. Vanslyke, Applied Physics Letters **51**, 913 (1987).
[2] L. Xiao, S. J. Su, Y. Agata, H. Lan, and J. Kido, Advanced Materials **21**, 1271 (2010).
[3] H. Uoyama, K. Goushi, K. Shizu, H. Nomura, and C. Adachi, Nature **492**, 234 (2012).
[4] C. Adachi, M. A. Baldo, M. E. Thompson, and S. R. Forrest, Journal of Applied Physics **90**, 5048 (2001).
[5] J. H. Lee, S. H. Cheng, S. J. Yoo, H. Shin, J. H. Chang, C. I. Wu, K. T. Wong, and J. J. Kim, Advanced Functional Materials **25**, 361 (2015).
[6] X. K. Liu, Z. Chen, C. J. Zheng, M. Chen, W. Liu, X. H. Zhang, and C. S. Lee, Advanced Materials. **27**, 2025 (2015).
[7] L. Mu, Z. Hu, Z. Zhong, C. Jiang, J. Wang, J. Peng, and Y. Cao, Organic Electronics **51**, 308 (2017).
[8] S. Wang, X. Wang, B. Yao, B. Zhang, J. Ding, Z. Xie, and L. Wang, Scientific Reports **5**, 1 (2015).
[9] D. Y. Chung, J. Huang, D. D. C. Bradley, and A. J. Campbell, Organic Electronics **11**, 1088 (2010).
[10] D. A. Pardo, G. E. Jabbour, and N. Peyghambarian, Advanced Materials **12**, 1249 (2000).
[11] A. Teichler, J. Perelaer, and U. S. Schubert, Journal of Materials Chemistry C **1**, 1910 (2013).
[12] M. Singh, H. M. Haverinen, P. Dhagat, and G. E. Jabbour, Advanced Materials **22**, 673 (2010).
[13] B. Geffroy, P. L. Roy, and C. Prat, Polymer International **55**, 572 (2006).
[14] W. F. Feehery, Sid Symposium Digest of Technical Papers **38**, 1834 (2007).
[15] E. I. Haskal, M. Buechel, J. F. Dijksman, P. C. Duineveld, E. A. Meulenkamp, C. A. H. A. Mutsaers, A. Sempel, P. Snijder, S. I. E. Vulto, P. van de Weijer, and S. H. P. M. de Winter, Sid Symposium Digest of Technical Papers **33**, 776 (2002).
[16] J. Rhee, J. Wang, S. Cha, J. Chung, D. Lee, S. Hong, B. Choi, J. Goh, K. Jung, and S. Kim, Sid Symposium Digest of Technical Papers **37**, 895 (2006).
[17] G.-J. A. H. Wetzelaer, D. Hartmann, S. G. Santamaría, M. Perez-Morales, A. S. Portillo, M. Lenes, W. Sarfert, and H. J. Bolink, Organic Electronics **12**, 1644 (2011).
[18] R. Xing, S. Wang, B. Zhang, X. Yu, J. Ding, L. Wang, and Y. Han, Rsc Advances **7**, 7725 (2017).
[19] A. M. Nardes, M. Kemerink, R. A. J. Janssen, J. A. M. Bastiaansen, N. M. M. Kiggen, B. M. W. Langeveld, A. J. J. M. van Breemen, and M. M. de Kok, Advanced Materials **19**, 1196 (2007).
[20] W. Zhang, H. Wang, J. Miao, Y. Zhu, M. U. Ali, T. Xu, L. Zhao, D. Zhang, G. He, and H. Meng, Organic Electronics **59**, 301 (2018).
[21] M. Kano, T. Minari, and K. Tsukagoshi, Applied Physics Letters **94**, 143304 (2009).
[22] Z. Z. You and J. Y. Dong, Applied Surface Science **253**, 2102 (2006).
[23] Y. J. Lee, S. S. Park, J. Kim, and H. Kim, Applied Physics Letters **94**, 223305 (2009).
[24] C. W. Miller, Z. P. Li, J. Akerman, and I. K. Schuller, Applied Physics Letters **90**, 043513 (2007).